

Supplementary Materials for

South Asian summer monsoon projections constrained by the interdecadal Pacific oscillation

Xin Huang, Tianjun Zhou*, Aiguo Dai, Hongmei Li, Chao Li, Xiaolong Chen, Jingwen Lu, Jin-Song Von storch, Bo Wu

*Corresponding author. Email: zhoutj@lasg.iap.ac.cn

Published 13 March 2020, *Sci. Adv.* **6**, eaay6546 (2020)

DOI: 10.1126/sciadv.aay6546

This PDF file includes:

Fig. S1. Evaluation of the historical SASM rainfall in MPI-ESM.

Fig. S2. IPO indices and the associated SST anomalies.

Fig. S3. The leading intermember EOF pattern of the SASM rainfall trends and the associated SST trend.

Fig. S4. Trends of IPO indices.

Fig. S5. Analogs among the 100 MPI-ESM ensemble members based on the IPO index trends.

Fig. S6. The influence of IPO evolution on the SASM rainfall trends projection uncertainty under the RCP4.5 scenario.

Fig. S7. The influence of IPO transition on the SASM rainfall trends projection uncertainty during 2016–2030 under the RCP8.5 scenario.

Fig. S8. The trend uncertainty in the SASM rainfall and the associated SST trends under the RCP8.5 scenario in CanESM2.

Fig. S9. AMO-related SASM rainfall and SST anomalies in the observations and MPI-ESM.

Fig. S10. SASM rainfall trend during 2016–2045 under the RCP8.5 scenario without influences of the AMO.

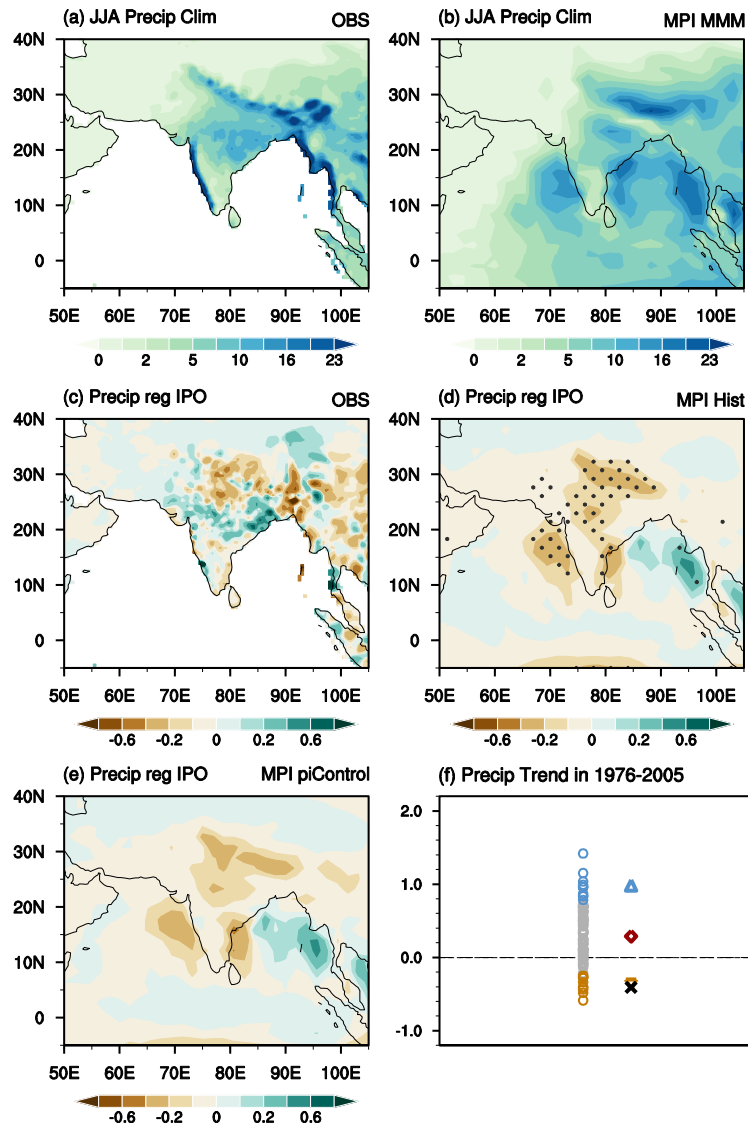


Fig. S1. Evaluation of the historical SASM rainfall in MPI-ESM. Climatological JJA mean rainfall over the SASM region during 1961-1999 for (A) GPCC v7 and (B) ensemble mean of the MPI-ESM. (C) The regressed 9-year running mean JJA rainfall from the GPCC v7 with respect to the observed IPO index from the ERSST v4 during 1920-2005. (D) The ensemble mean of the regressed 9-year running mean JJA rainfall onto the IPO index within each ensemble member during 1920-2005. (E) The regressed 9-year running mean JJA rainfall onto the IPO index from 1000-year MPI-ESM preindustrial control run. Stippling denotes 80 out of the 100 ensemble members agreement in signs. Units: mm day^{-1} . (F) The SASM rainfall trends for the GPCC v7 (black cross) and the 100 MPI-ESM members (circles) during 1976-2005 (units: $\text{mm day}^{-1} (30\text{yr})^{-1}$). The 10 members with the wettest (driest) trends are shown in blue (brown) circles. The diamonds, blue triangles, brown inverse triangles denote the ensemble mean of the 100 members, the 10 wettest and the 10 driest members respectively.

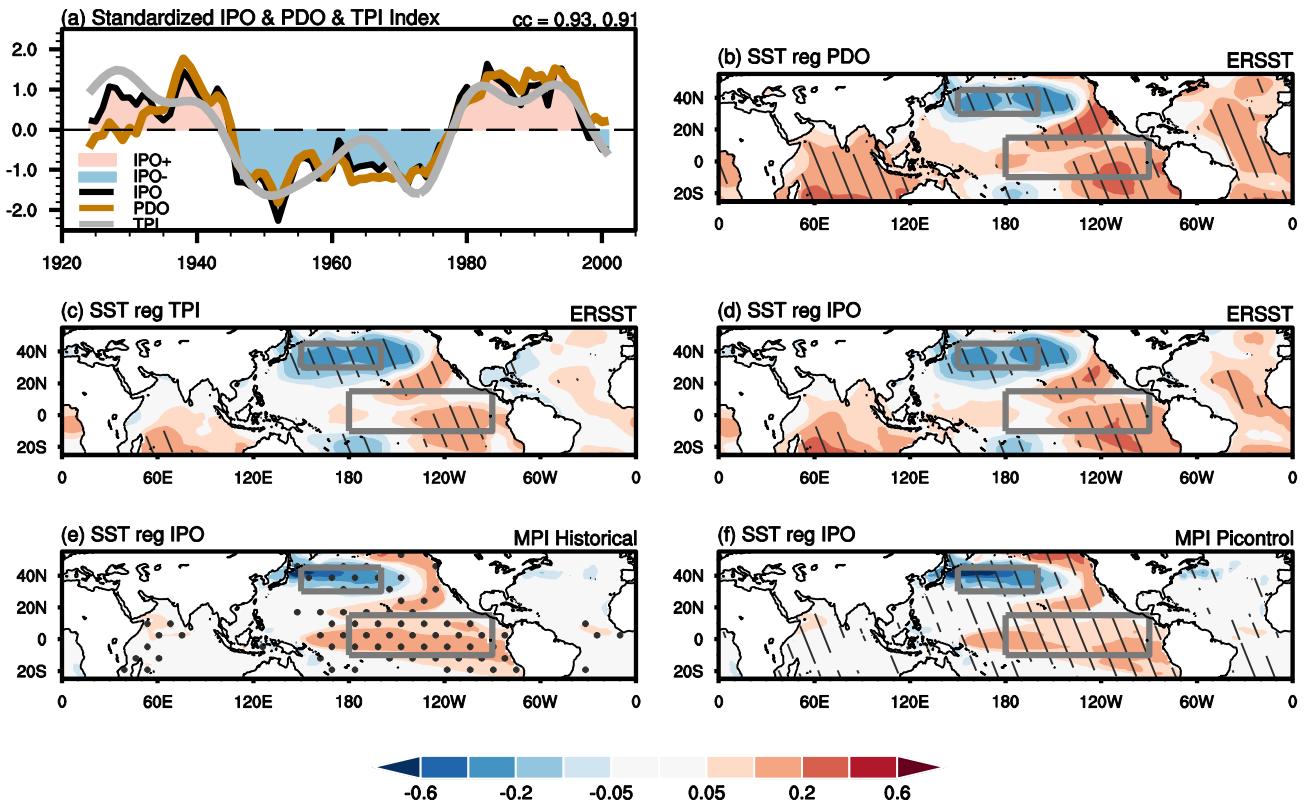


Fig. S2. IPO indices and the associated SST anomalies. (A) The standardized time series of the observed IPO index (defined as the 9-year running mean SST gradients between TCEP and NP, positive in red and negative in blue), the standardized 9-year running mean PDO (orange) and TPI (grey) indices. The correlation coefficient between the IPO and the PDO and the TPI indices are 0.93 and 0.91 ($p < 0.01$), respectively, during 1920-2005. The regressed 9-year running mean JJA SST anomalies from the ERSST v4 (units: K) with respect to the standardized 9-year running mean (B) PDO index, (C) TPI index and (D) IPO index during 1920-2005. (E) The ensemble mean of the regressed 9-year running mean JJA SST with respect to the standardized IPO index within each member during 1920-2005. (F) The regressed 9-year running mean JJA SST anomalies with respect to the IPO index from the 1000-year MPI-ESM preindustrial control run. Slant hatching in (B-D) and (F) denotes regression coefficients significant at the 95% confidence level. Stippling in (E) denotes 80 out of the 100 ensemble members agreement in signs.

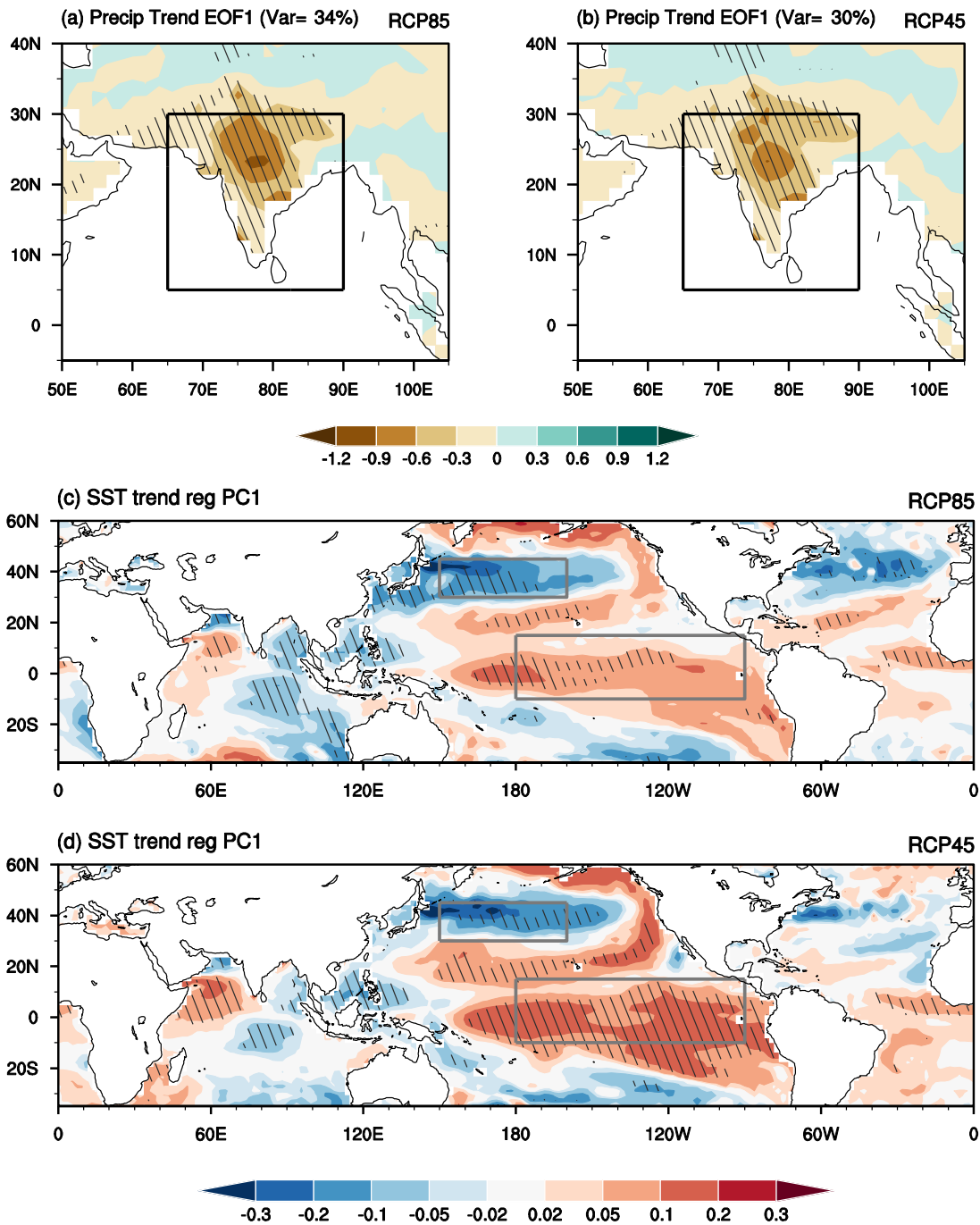


Fig. S3. The leading intermember EOF pattern of the SASM rainfall trends and the associated SST trend. An EOF analysis was applied to the 100 JJA land rainfall trend maps over the SASM domain (5°N-30°N, 65°E-90°E) with the member index here serving as the time index in a conventional EOF analysis. (A-B) show the leading EOF pattern (units: mm day⁻¹ (30yr)⁻¹) under the (A) RCP8.5 and (B) RCP4.5 scenarios. (C-D) are the regression pattern of the SST trends across 100 members through the member index. The leading modes explain 34% and 30% of the SASM rainfall trend variance for the RCP8.5 and RCP4.5 scenarios, respectively.

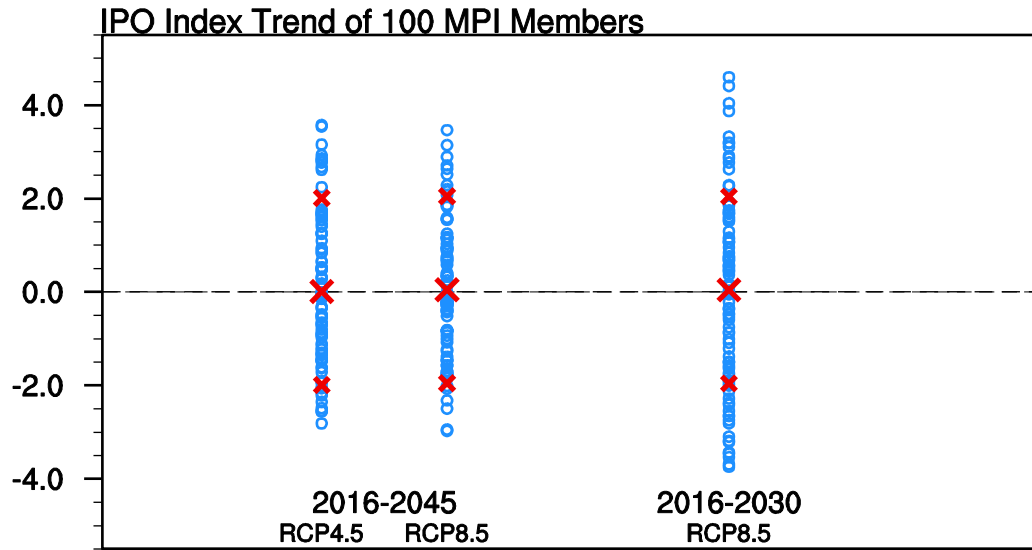


Fig. S4. Trends of IPO indices. Each blue circle represents a trend of the standardized IPO index (units: $(30\text{yr})^{-1}$) from one of the 100 members of MPI-ESM during 2016-2045 (left) under the RCP4.5 and RCP8.5 scenario, and during 2016-2030 (right) under the RCP8.5 scenario. The larger red crosses denote the ensemble mean of the 100 members, and the smaller red crosses denote the trends of $\pm 2 \text{ SD } (30 \text{ yr})^{-1}$, which are used to represent a significant positive or negative IPO phase transition in the study.

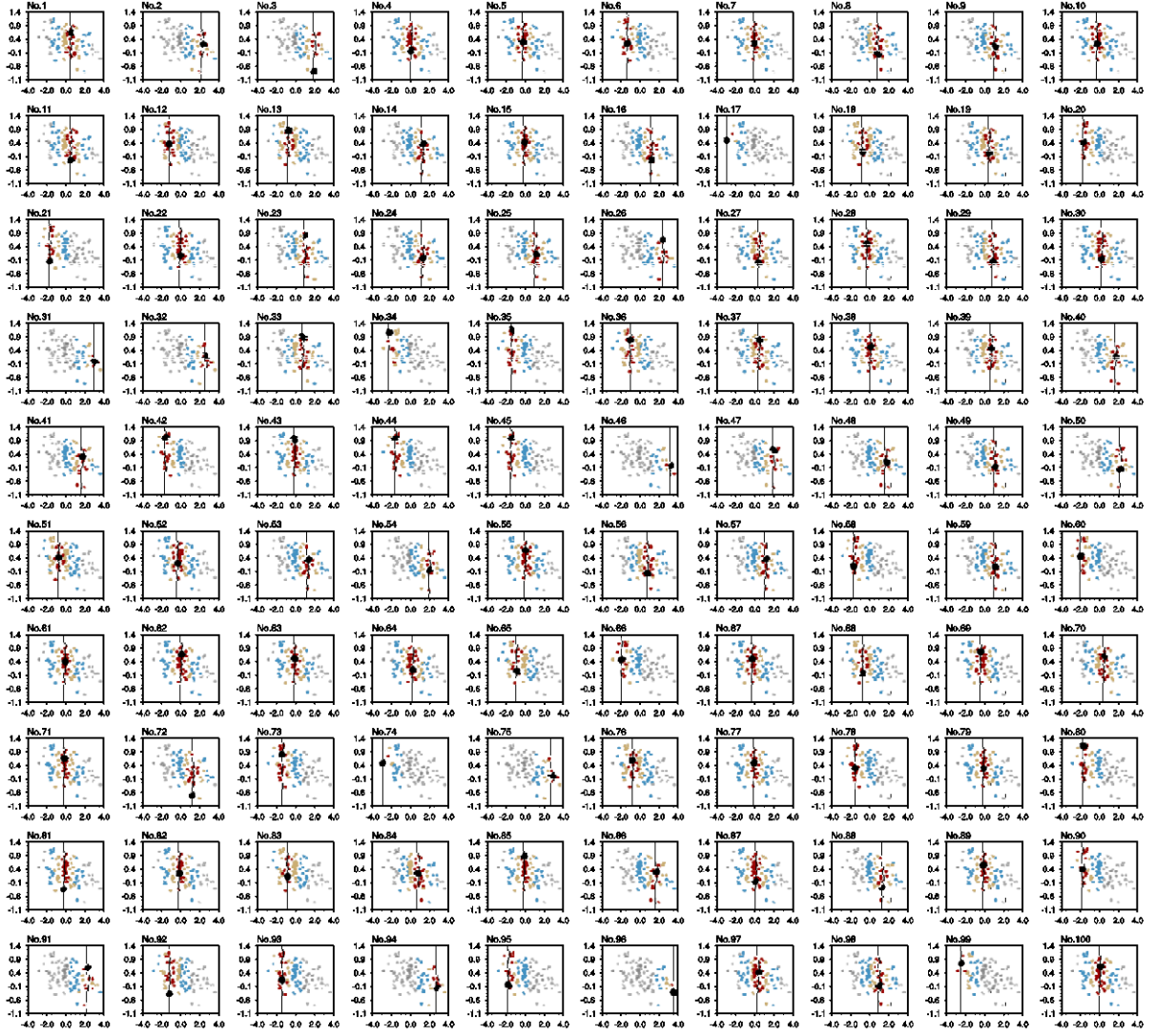


Fig. S5. Analogs among the 100 MPI-ESM ensemble members based on the IPO index trends. Scatterplot between the standardized IPO index trends (x-axis, units: $(30 \text{ yr})^{-1}$) and the SASM rainfall trends (y-axis, units: $\text{mm day}^{-1} (30 \text{ yr})^{-1}$) among the MPI-ESM 100 members during 2016-2045 under the RCP8.5 scenario, same as **Fig. 2C**. The black dot in each figure denotes the reference member (member i) for each case, with the black line highlighting its IPO index trend ($\frac{\partial \text{IPO}(i,t)}{\partial t}$). The red dots represent the selected members a in the Group A for each case which have standardized IPO index trends within the range of $(\frac{\partial \text{IPO}(i,t)}{\partial t} - 0.5) < \frac{\partial \text{IPO}(a,t)}{\partial t} < (\frac{\partial \text{IPO}(i,t)}{\partial t} + 0.5)$ $(30 \text{ year})^{-1}$. The yellow dots represent the selected members b in the Group B which have standardized IPO index trends within the range of $(\frac{\partial \text{IPO}(i,t)}{\partial t} - 1.0) < \frac{\partial \text{IPO}(b,t)}{\partial t} < (\frac{\partial \text{IPO}(i,t)}{\partial t} + 1.0)$ $(30 \text{ year})^{-1}$. The blue dots represent the selected members c in the Group C which have standardized IPO index trends within the range of $(\frac{\partial \text{IPO}(i,t)}{\partial t} - 2.0) < \frac{\partial \text{IPO}(c,t)}{\partial t} < (\frac{\partial \text{IPO}(i,t)}{\partial t} + 2.0)$ $(30 \text{ year})^{-1}$.

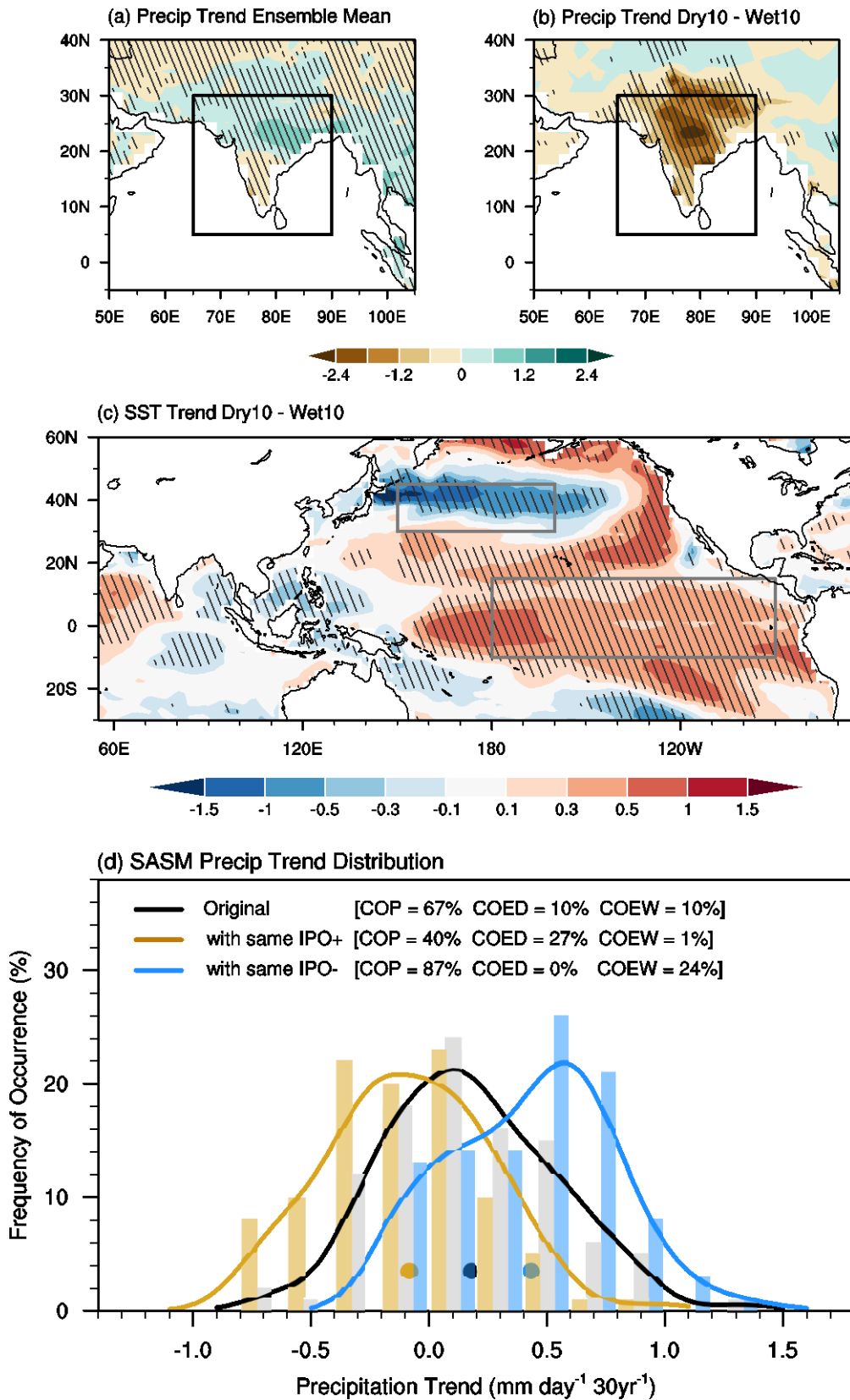


Fig. S6. The influence of IPO evolution on the SASM rainfall trends projection uncertainty under the RCP4.5 scenario. June-July-August (JJA) mean rainfall trends under the RCP4.5 scenario during 2016-2045 for (A) MPI-ESM 100-member ensemble mean, (B) the mean trend differences between the 10 members with the

driest and the wettest trends. Units: $\text{mm day}^{-1} (30\text{yr})^{-1}$. The boxes in (A-B) highlight the SASM region (5°N - 30°N , 65°E - 90°E). (C) SST trend differences during 2016-2045 under the RCP4.5 scenario between the 10 driest and 10 wettest members of MPI-ESM (units: $\text{K} (30 \text{ yr})^{-1}$). Slant hatching denotes trends significant at the 95% confidence level. (D) Histograms (bars) and 100-bins fitted distribution (lines) of the area-averaged SASM rainfall trends derived from the 100 MPI-ESM ensemble members. The grey bars and the black fitted curve show the frequency of occurrence of the rainfall trends in the model output. The brown and blue histograms and fitted curves show the frequency of occurrence of the area-averaged rainfall trends with the same amplitude of a positive ($+2 (30 \text{ yr})^{-1}$) or a negative ($-2 (30 \text{ yr})^{-1}$) IPO phase transition, respectively, from 2016-2045 under the RCP4.5 scenario. The black, brown and blue dots denote the ensemble mean of the distribution with the corresponding color.

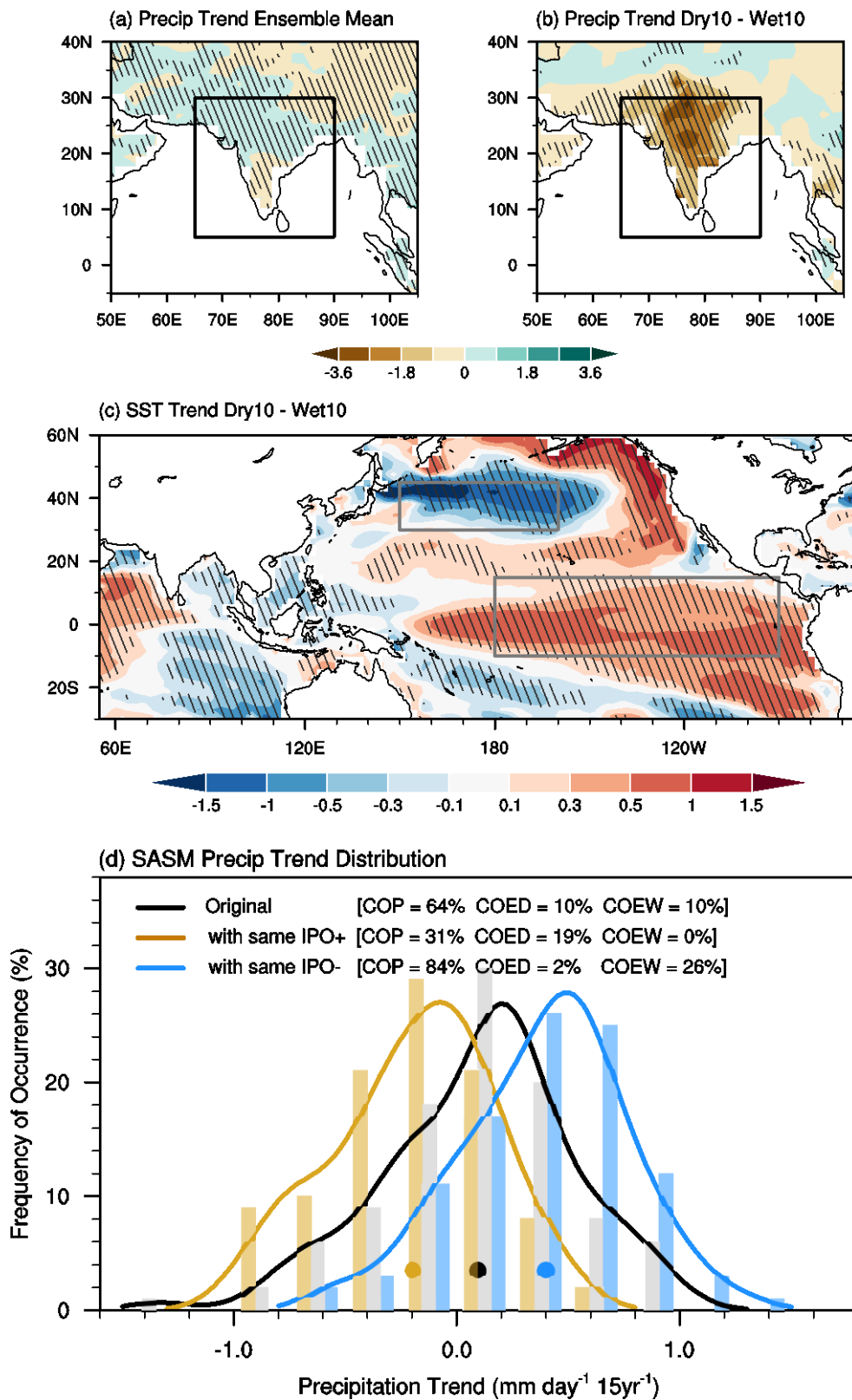


Fig. S7. The influence of IPO transition on the SASM rainfall trends projection uncertainty during 2016–2030 under the RCP8.5 scenario. Same as Figure S5 but for rainfall and sea surface temperature trends during 2016-2030 under the RCP8.5 scenario.

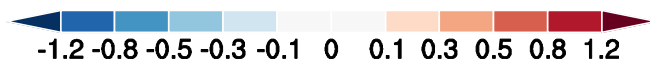
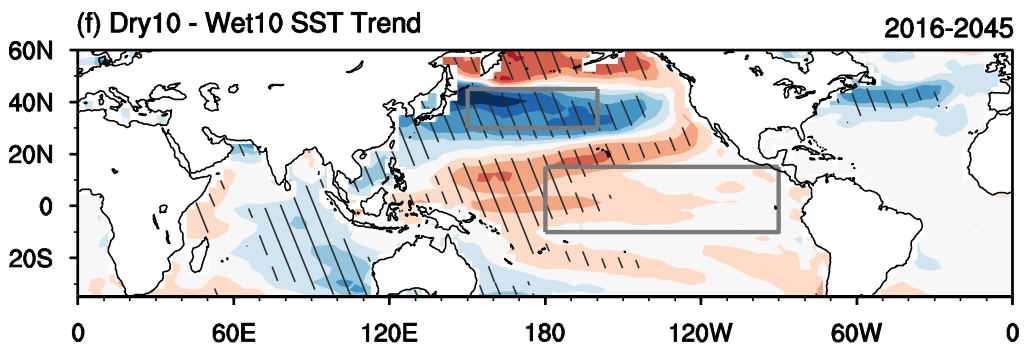
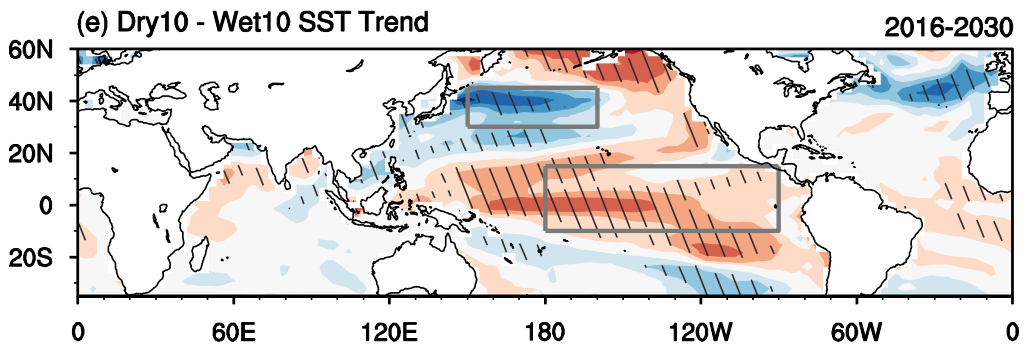
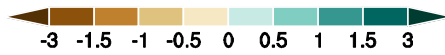
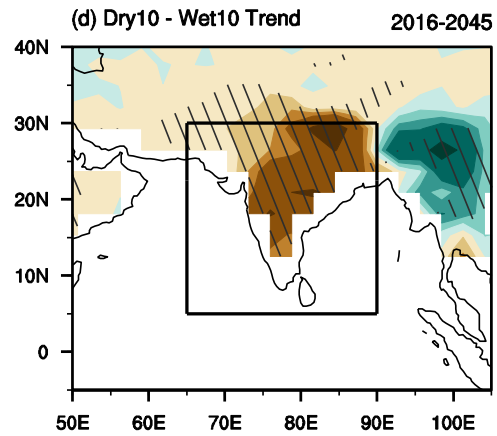
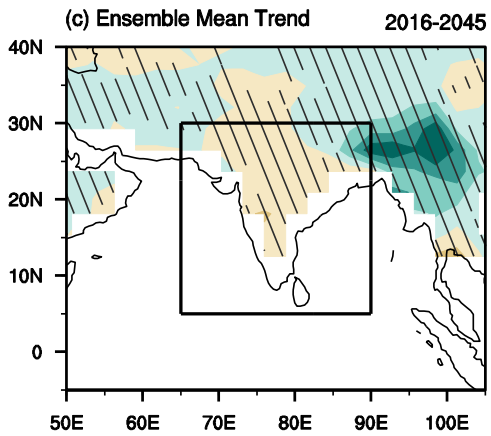
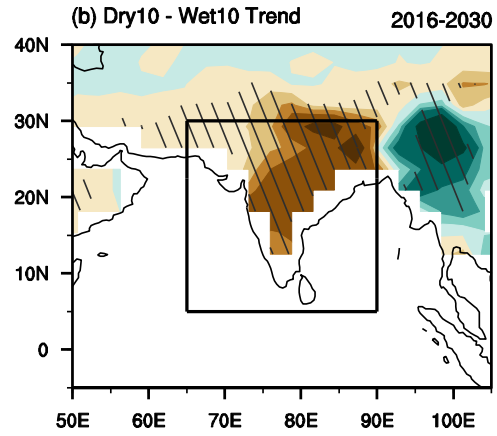
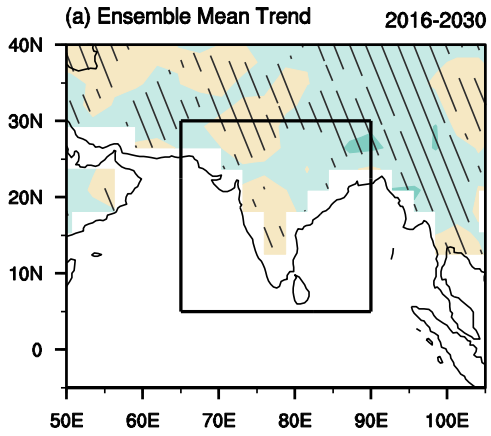


Fig. S8. The trend uncertainty in the SASM rainfall and the associated SST trends under the RCP8.5 scenario in CanESM2. June-July-August (JJA) mean rainfall trends under the RCP8.5 scenario during 2016-2030 for (A) CanESM2 50-member ensemble mean, (B) the mean trend differences between the 10 members with the driest and the wettest trends. Units: $\text{mm day}^{-1} (15\text{yr})^{-1}$. (E) SST trend differences during 2016-2030 under the RCP8.5 scenario between the 10 driest and 10 wettest members of CanESM2 (units: $\text{K} (15 \text{ yr})^{-1}$). C., D. and F. are same as A., B. and E. but for 2016-2045. Slant hatching denotes regions significant at the 95% confidence level.

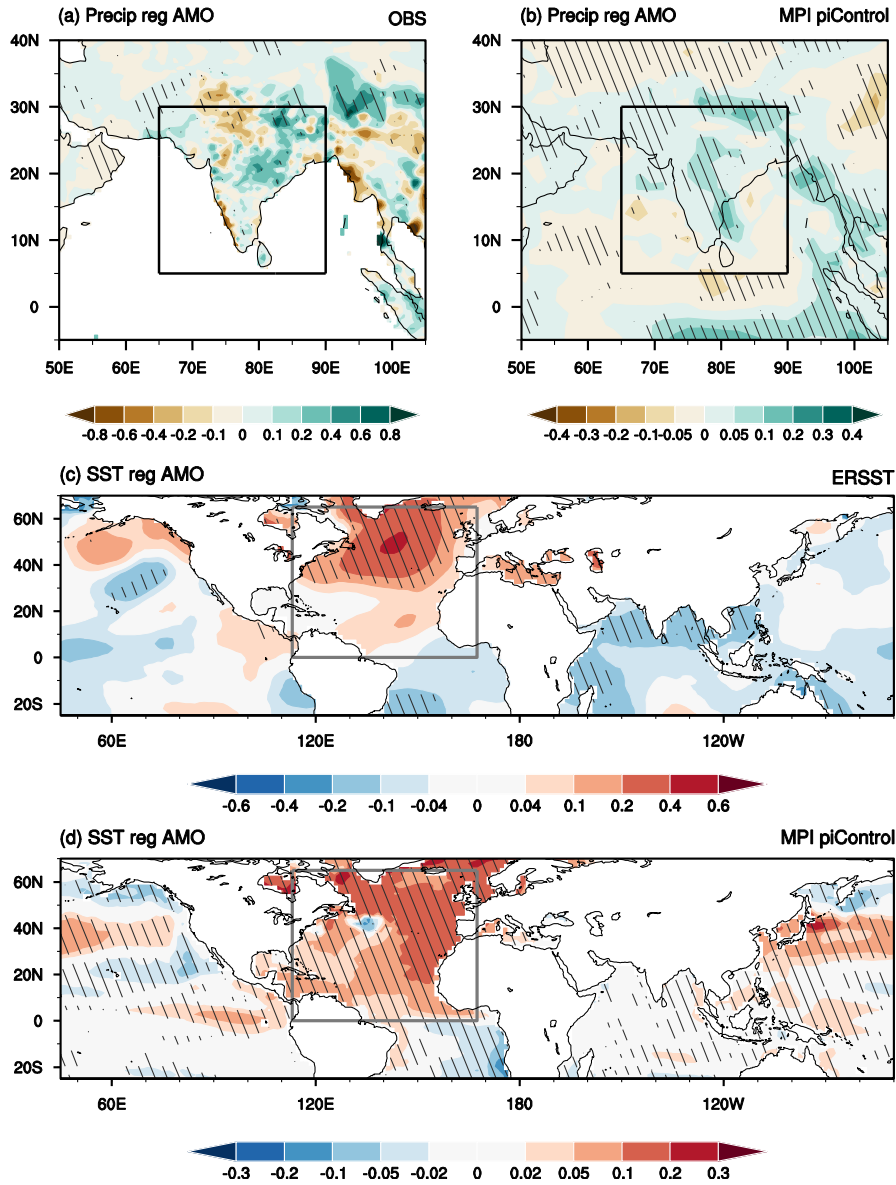


Fig. S9. AMO-related SASM rainfall and SST anomalies in the observations and MPI-ESM. **(A)** The regressed 9-year running mean JJA rainfall from the GPCP v7 with respect to the observed AMO index (defined as the 9-year running mean area-averaged SST anomalies over the North Atlantic Ocean after subtracting the global-mean SST anomaly time series) from the ERSST v4 during 1920-2005 (units: mm day⁻¹). **(B)** The regressed 9-year running mean JJA rainfall onto the AMO index from 1000-year MPI-ESM preindustrial control run (units: mm day⁻¹). **(C)** The regressed 9-year running mean JJA SST anomalies from the ERSST v4 with respect to the standardized 9-year running mean AMO index during 1920-2005 (units: K). **(D)** The regressed 9-year running mean JJA SST anomalies with respect to the IPO index from the 1000-year MPI-ESM preindustrial control run (units: K). Slant hatching denotes regression coefficients significant at the 95% confidence level.

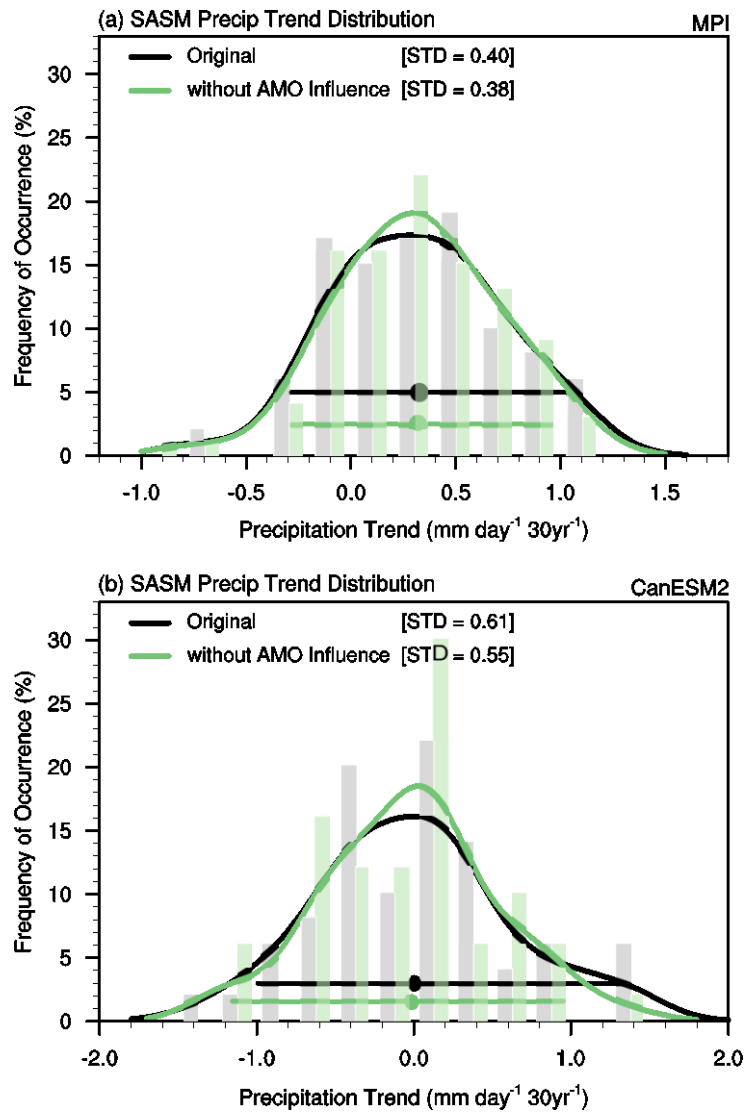


Fig. S10. SASM rainfall trend during 2016–2045 under the RCP8.5 scenario without influences of the AMO. Histograms and 100-bins fitted distribution of the area-averaged SASM rainfall trends derived from the (A) 100 MPI-ESM ensemble members, (B) 50 CanESM2 ensemble members. The grey bars and the black fitted curves are the same as Fig. 3A and Fig. 4B. The green bars and fitted curves show the frequency of occurrence of the area-averaged rainfall trends with the influence of the AMO being removed through linear regression against the standardized AMO index during 1950–2099 in the individual runs (with a standard deviation of 0.38 and 0.55 in MPI-ESM and CanESM2, respectively). The black and green dots denote the ensemble mean of the distribution represented by the corresponding color. The black and green horizontal lines denote the 5th to 95th percentile range of the distribution represented by the corresponding colors.